Supramolecular Photochemistry and Photophysics. A Cylindrical Macrotricyclic Receptor and Its Adducts with Protons, Ammonium Ions, and a Pt(II) Complex

Roberto Ballardini,*[1a] Vincenzo Balzani,*[1b] Alberto Credi,[1b] Maria Teresa Gandolfi,[1b] Florence Kotzyba-Hibert,[1c] Jean-Marie Lehn,*[1c] and Luca Prodi[1b]

Contribution from the Istituto FRAE-CNR, 40126 Bologna, Italy, Dipartimento di Chimica "G. Ciamician", Università di Bologna, 40126 Bologna, Italy, and Institut Le Bel, Université Louis Pasteur, 67000 Strasbourg, France

Received January 25, 1994®

Abstract: The absorption spectrum and the luminescence properties of a cylindrical macrotricyclic receptor (**1**), which is made of two diazatetraoxa macrocyclic [18]-N_2O_4 units linked by two 2,6-dimethylnaphthalene (DMN) bridges, have been investigated. Comparison with the behavior of the 2,6-dimethylnaphthalene reference chromophore shows that in CH_2Cl_2 solution at room temperature, the covalent bond between the DMN units and the nonabsorbing and nonemitting [18]-N_2O_4 macrocycles causes the appearance of a charge-transfer (CT) absorption tail below 310 nm, the disappearance of the structured DMN fluorescence at 342 nm, and the appearance of a broad and weak CT emission band at 438 nm. In rigid matrix at 77 K, however, **1** behaves similarly to DMN, showing a structured fluorescence band with maximum at 342 nm and a structured phosphorescence band with maximum at 518 nm and τ = 2.6 s. Addition of CF_3COOH to a CH_2Cl_2 solution of **1** causes the successive protonation of the four amine units of the two [18]-N_2O_4 macrocycles which are responsible for the CT transitions to the naphthalene rings. As a consequence, the CT absorption tail disappears, the absorption spectrum of the macrotricycle becomes very similar to that exhibited by the isolated DMN chromophore, and the DMN-type fluorescence reappears. The luminescence intensity at 342 nm increases by at least 800 times upon protonation. Therefore, **1** is a fluorescence sensor highly responsive to protons. Upon adduct formation with α,ω-alkanediyldiammonium ion $NH_3^+(CH_2)_5NH_3^+$ (cadaverine cation), for which a molecular inclusion into the receptor **1** was previously demonstrated, the intensities of the CT absorption tail below 310 nm and the CT luminescence band at 438 nm decrease by ~50%, but the fluorescence DMN band at 342 nm is negligibly small. Similar results are obtained upon adduct formation with NH_4^+ ions. The $[Pt(NH_3)_2(bpy)]^{2+}$ complex, which can be used as a guest for a variety of crown ethers, forms a 1:1 adduct with unprotonated **1**. The absorption spectrum of the adduct is noticeably different from that expected for the sum of the two separated components, particularly because of the presence of an absorption in the 340–420-nm region. At room temperature, the luminescence bands exhibited by the two separated components are no longer observed in the adduct. In rigid matrix at 77 K, the phosphorescence band of **1** can be observed in the adduct regardless of the excitation wavelength, but its lifetime (0.8 ms) is considerably shorter than that (2.6 s) of the phosphorescence of **1**. As suggested by observation of CPK models, the above results indicate that $[Pt(NH_3)_2(bpy)]^{2+}$ is hosted in the cylindrical cavity of **1** with an amine ligand which interacts with a [18]-N_2O_4 macrocycle unit via hydrogen bonds and the $Pt(bpy)^{2+}$ electron-deficient moiety involved in a CT interaction with the DMN chromophoric units.

Introduction

In the past few years, there has been an increasing interest in the photophysics and photochemistry of supramolecular species for both basic and applicative reasons.[2-10] In host–guest systems, the photochemical and photophysical properties of each partner can be profoundly modified on adduct formation. Such changes can be useful for obtaining information on the structure of the adduct and, at the same time, for designing photochemical molecular devices for a variety of light-induced functions.

Marked effects of protonation, metal ion binding, and diammonium substrate binding on luminescence properties have been observed for macrobicyclic[11] and macrotricyclic[12] receptors incorporating anthracene groups.

The cylindrical macrotricyclic receptor **1**,[12] which is made of two diazatetraoxa macrocyclic [18]-N_2O_4 units linked by two 2,6-dimethylnaphthalene bridges, can encapsulate selectively α,ω-alkanediyldiammonium ions of compatible length,[12] as is also the case for similar macrotricyclic[13] or bis-macrocyclic[14] receptors based on anthracene. **1** is expected to be an interesting host for photophysical studies because of its cylindrical cavity, the two

• Abstract published in *Advance ACS Abstracts,* May 15, 1994.

(1) (a) FRAE-CNR Institute, Bologna, Italy. (b) University of Bologna, Italy. (c) University of Strasbourg, France.

(2) *Supramolecular Photochemistry*; Balzani, V., Ed.; Reidel: Dordrecht, The Netherlands, 1987.

(3) Lehn, J.-M. *Angew. Chem., Int. Ed. Engl.* **1988**, *27*, 89.

(4) Lehn, J.-M. *Angew. Chem., Int. Ed. Engl.* **1990**, *29*, 1304.

(5) Balzani V.; Scandola, F. *Supramolecular Photochemistry*; Horwood: Chichester, U.K., 1991.

(6) *Frontiers in Supramolecular Organic Chemistry and Photochemistry*; Schneider, H. J., Dürr, H., Eds.; VCH: Weinheim, Germany, 1991.

(7) Vögtle, F. *Supramolecular Chemistry*; Wiley: Chichester, U.K., 1991.

(8) Balzani, V. *Tetrahedron* **1992**, *48*, 10443.

(9) Bissell, R. A.; de Silva, A. P.; Gunaratne, H. Q. N.; Lynch, P. L. M.; Maguire, G. E. M.; Sandanayake, K. R. A. S. *Chem. Soc. Rev.* **1992**, 187.

(10) Desvergne, J.-P.; Fages, F.; Bouas-Laurent, H.; Marsau, P. *Pure Appl. Chem.* **1992**, *64*, 1231.

(11) Fages, F.; Desvergne, J.-P.; Bouas-Laurent, H.; Marsau, P.; Lehn, J.-M.; Kotzyba-Hibert, F.; Albrecht-Gary, A.-M.; Al-Joubbeh, M. *J. Am. Chem. Soc.* **1989**, *111*, 8672.

(12) (a) Kotzyba-Hibert, F.; Lehn, J.-M.; Vierling, P. *Tetrahedron Lett.* **1980**, *21*, 941. (b) Pascard, C.; Riche, C.; Cesario, M.; Kotzyba-Hibert, F.; Lehn, J.-M. *J. Chem. Soc., Chem. Commun.* **1982**, 557.

(13) (a) Fages, F.; Desvergne, J.-P.; Bouas-Laurent, H.; Lehn, J.-M.; Konopelski, J. P.; Marsau, P.; Barrans, Y. *J. Chem. Soc., Chem. Commun.* **1990**, 655. (b) Fages, F.; Desvergne, J.-P.; Kampe, K.; Bouas-Laurent, H.; Lehn, J.-M.; Meyer, M.; Albrecht-Gary, A.-M. *J. Am. Chem. Soc.* **1993**, *115*, 3658.

(14) de Silva, A. P.; Sandanayake, K. R. A. S. *Angew. Chem., Int. Ed. Engl.* **1990**, *29*, 1173.

0002-7863/94/1516-5741$04.50/0

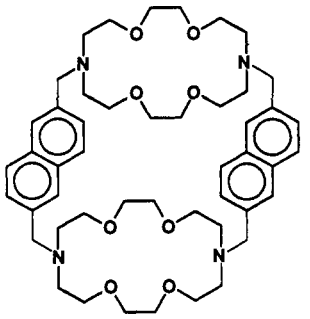

1

potentially luminescent naphthalene units, and the amine groups contained in the two [18]-N_2O_4 macrocycles.

The $[Pt(NH_3)_2(bpy)]^{2+}$ complex (bpy = 2,2′-bipyridine) is known to form adducts with crown ethers because its ammonia ligands give rise to hydrogen bonds with their oxygen sites.[15] Furthermore, it has been shown that this complex exhibits characteristic absorption, emission, and photochemical properties that can be strongly modified upon π–π interaction between the $Pt(bpy)^{2+}$ moiety and aromatic rings.[16] CPK molecular models suggest that $[Pt(NH_3)_2(bpy)]^{2+}$ can be encapsulated into the macrotricyclic receptor **1**. This has prompted us to investigate the photophysical behavior of **1** and the adduct of **1** with $[Pt(NH_3)_2(bpy)]^{2+}$. In order to better understand the properties of the receptor **1**, we have also investigated its photophysical behavior on protonation of the amine groups and on adduct formation with NH_4^+ and $NH_3^+(CH_2)_5NH_3^+$ (cadaverine cation). In doing that, we have found that **1** is an excellent fluorescent sensor responsive to protons.[17-19]

Experimental Section

Chemicals. The receptor **1** and its [18]-N_2O_4 component were available from previous investigations.[12] The synthesis of $[Pt(NH_3)_2(bpy)](PF_6)_2$ has already been described.[16b] 2,6-Dimethylnaphthalene (DMN) and cadaverine chlorohydrate $(NH_3(CH_2)_5NH_3)Cl_2$ were obtained from Aldrich. Dichloromethane and trifluoroacetic acid were Merck products. The former was distilled on P_2O_5 before use to remove water traces.

Equipment. Absorption spectra were recorded with a Perkin-Elmer λ6 spectrophotometer. Uncorrected emission spectra and corrected excitation spectra were obtained with a Perkin-Elmer LS50 spectrofluorimeter, which was also used to obtain phosphorescence lifetimes in the 10-μs to 5-s time region. In order to allow comparison of emission intensities, corrections for the different absorbance and phototube sensitivity were performed when necessary. An Edinburgh single-photon counting apparatus[16b] was used for shorter lifetimes. Emission spectra at 77 K were obtained in CH_2Cl_2 matrix or MeOH/EtOH (4:1, v/v). Degassed solutions were obtained by the freeze–thaw–pump method. All the experiments were performed in CH_2Cl_2 at room temperature (~25 °C) unless otherwise noted.

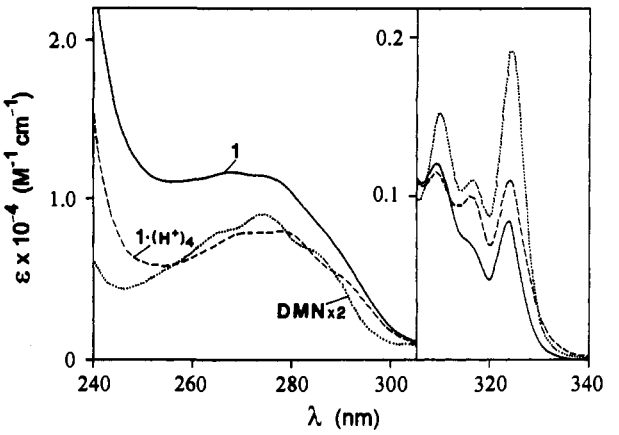

Figure 1. Absorption spectra in CH_2Cl_2 solution at room temperature of **1**, **1**·$(H^+)_4$, and 2,6-dimethylnaphthalene (DMN). For comparison purposes, the molar absorption coefficient of the last compound has been multiplied by a factor of 2.

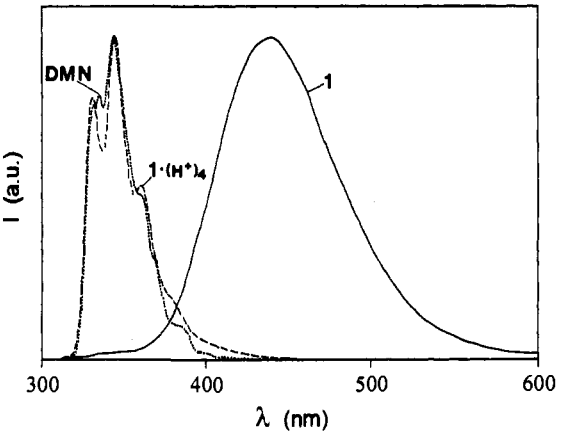

Figure 2. Luminescence spectra in CH_2Cl_2 solution at room temperature of **1**, **1**·$(H^+)_4$, and 2,6-dimethylnaphthalene (DMN).

Results and Discussion

Receptor 1, a Fluorescent Sensor Responsive to Protons. The absorption spectrum of **1** is shown in Figure 1. For comparison purposes, the spectrum of 2,6-dimethylnaphthalene (DMN) is also shown. The other component of **1**, i.e., the macrocycle [18]-N_2O_4, shows a negligible absorption in the spectral region examined ($\epsilon < 20$ M^{-1} cm^{-1} at $\lambda_{max} = 267$ nm). Comparison between the spectrum of **1** with the summation of the spectra of its components (i.e., with twice the absorption spectrum of DMN, Figure 1) shows that bonding with two [18]-N_2O_4 units causes the appearance of an absorption tail in the UV region and small changes in the structure and intensity of the ^1L_b ($\lambda_{max} = 323$ nm) and ^1L_a ($\lambda_{max} = 274$ nm) $\pi \rightarrow \pi^*$ bands of DMN. The absorption tail (as well as the corresponding luminescence band, vide infra) can be assigned to CT transitions from the nonbonding orbital of the amine groups of the [18]-N_2O_4 macrocycles to the π^* orbitals of the naphthalene units. This assignment is confirmed by the disappearance of the absorption tail upon addition of 4 equiv of trifluoroacetic acid which, as will be discussed in more detail later on, causes full protonation of the amine groups of the two [18]-N_2O_4 units (Figure 1). The small differences observed between the absorption spectrum of **1**·$(H^+)_4$ and DMN can be attributed to perturbation of the π–π^* naphthalene transitions by the nearby proton charges in **1**·$(H^+)_4$ (vide infra).

Figure 2 shows the luminescence spectra of **1**, **1**·$(H^+)_4$, and DMN in CH_2Cl_2 at room temperature. The [18]-N_2O_4 macrocycle does not show any luminescence. As one can see, **1**·$(H^+)_4$

(15) Colquhoun, H. M.; Stoddart, J. F.; Williams, D. J. *Angew. Chem., Int. Ed. Engl.* **1986**, *25*, 487.

(16) (a) Ballardini, R.; Gandolfi, M. T.; Balzani, V.; Kohnke, F. H.; Stoddart, J. F. *Angew. Chem., Int. Ed. Engl.* **1988**, *27*, 692. (b) Ballardini, R.; Gandolfi, M. T.; Prodi, L.; Ciano, M.; Balzani, V.; Kohnke, F. H.; Shahriari-Zavareh, H.; Spencer, N.; Stoddart, J. F. *J. Am. Chem. Soc.* **1989**, *111*, 7072. (c) Gandolfi, M. T.; Zappi, T.; Ballardini, R.; Prodi, L.; Balzani, V.; Stoddart, J. F.; Mathias, J. P.; Spencer, N. *Gazz. Chim. Ital.* **1991**, *121*, 521. (d) Ballardini, R.; Gandolfi, M. T.; Balzani, V.; Desvergne, J.-P.; Bouas-Laurent, H. *J. Phys. Chem.* **1991**, *95*, 2080. (e) Balzani, V.; Ballardini, R.; Gandolfi, M. T.; Prodi, L. In ref. 6, p 371.

(17) For reviews on fluorescent sensors, see refs 9 and 18. For some recent papers on proton-controlled fluorescence, see ref 19.

(18) (a) Czarnik, A. W. In ref 6, p 109. (b) Ueno, A.; Osa, T. In *Photochemistry in Organized and Constrained Media*; Ramamurthy, V., Ed.; VCH: New York, 1991; p 739. (c) Bissell, R. A.; de Silva, A. P.; Gunaratne, H. Q. N.; Lynch, P. L. M.; Maguire, G. E. M.; McCoy, C. P.; Sandanayake, K. R. A. S. *Top. Curr. Chem.*, in press.

(19) (a) Bissell, R. A.; Calle, E.; de Silva, A. P.; de Silva, S. A.; Gunaratne, H. Q. N.; Habib-Jiwan, J.-L.; Peiris, S. L. A.; Rupasinghe, R. A. D. D.; Samarasinghe, T. K. S. D.; Sandanayake, K. R. A. S.; Soumillion, J. P. *J. Chem. Soc., Perkin Trans.* **1992**, 1559. (b) de Silva, A. P.; Gunaratne, H. Q. N.; McCoy, C. P. *Nature* **1993**, *364*, 42. (c) Grigg, R.; Norbert, W. D. J. A. *J. Chem. Soc., Chem. Commun.* **1992**, 1298, 1300.

Table 1. Luminescence Properties[a]

	fluorescence, 293 K			phosphorescence, 77 K	
	λ_{max} (nm)	I_{rel}[b]	τ (ns)	λ_{max} (nm)	τ (s)
DMN	342	100	14	525[c]	1.8[c]
1	342	<0.1			
	438	8	2.6	518	2.6
1·$(H^+)_4$	344	108	28	528	1.7
1·$[NH_3(CH_2)_5NH_3]^{2+}$ [d,e]	340	2.6	11	512	1.5
	438	4.4	2		
1·$[Pt(NH_3)_2(bpy)]^{2+}$	no emission			520	8×10^{-4}
$[Pt(NH_3)_2(bpy)]^{2+}$	488[f]	1[f]	100[f]	486	2.5×10^{-5}

[a] In degassed CH_2Cl_2 solution, unless otherwise noted. [b] Relative quantum yields; quantum yield 0.26 for DMN, using naphthalene in cyclohexane as a standard (Φ = 0.23; Berlman, I. B. *Handbook of Fluorescence Spectra of Aromatic Molecules*; Academic Press: London, 1971). [c] In MeOH/EtOH (4:1, v/v). [d] In CH_2Cl_2/MeOH (10:1, v/v). [e] Very similar results have been obtained for the adduct with NH_4^+ ions at room temperature. [f] ^{3}LC bpy centered phosphorescence at room temperature, ref 16b.

behaves as the DMN reference compound, exhibiting the structured fluorescence band characteristic of the naphthalene chromophoric group. The luminescence lifetime (Table 1) is 14 ns for DMN and 28 ns for **1**·$(H^+)_4$ in degassed solution. The luminescence spectrum of **1**, however, is clearly different from that of DMN, since the structured band with maximum at 342 nm is replaced by an unstructured, broad band with maximum at 438 nm (τ = 2.6 ns). The maximum of the emission band moves to the red with increasing solvent polarity (λ_{max} = 457 nm in butyronitrile).

A behavior similar to that exhibited by **1** is also observed for 2,6-bis((*N*,*N*-dimethylamino)methyl)naphthalene[20] and *N*-*n*-butyl-*N*,*N*-bis(2-naphthylmethyl)ammine,[21] which can be considered as model compounds for the substituted (aminomethyl)-naphthalene moieties of **1**. In such compounds, the broad luminescence band, which disappears upon addition of acid,[20] was attributed to exciplex emission. Because of the presence of a CT absorption (vide supra) and in view of the greater rigidity of the macrotricyclic structure, we prefer to assign the broad luminescence band of **1** (Figure 2) to a CT emission[22] rather than to an exciplex emission. The excitation spectrum of **1** at λ_{em} = 438 nm matches well the absorption spectrum, showing that the luminescent CT level is reached with the same (presumably unitary) efficiency from the upper-lying levels.

The fluorescent behavior of **1** can be reversibly switched by addition of acid or base. In other words, **1** is a fluorescent sensor responsive to protons.[17-19] The sensitivity of this sensor is extremely high since the luminescence intensity at 344 nm increases by at least 800 times upon full protonation.

In rigid CH_2Cl_2 matrix at 77 K, DMN shows both a fluorescence and a phosphorescence band (Figure 3). Under such conditions, **1** behaves quite similarly to DMN, the only difference being a tail in the 360–460-nm region which is probably due to a residual CT emission.

The changes in the absorption and emission behavior of **1** upon protonation can be explained on the basis of the schematic potential energy curves shown in Figure 4. In the DMN reference chromophore, the relevant energy levels are the two lowest singlet excited states, S_1 (^1L_b) and S_2 (^1L_a), and the lowest triplet state T_1 (^3L_a), all of $\pi \rightarrow \pi^*$ orbital origin. S_1 and S_2 are responsible for the two absorption bands (Figure 1), S_1 is responsible for the fluorescence band (Figures 2 and 3), and T_1 is responsible for the

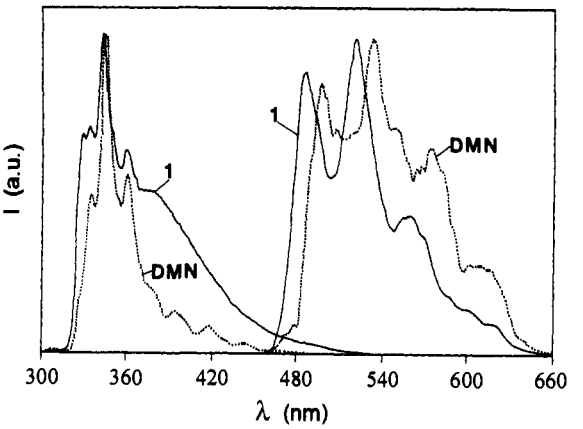

Figure 3. Fluorescence (left) and phosphorescence (right) spectra of **1** and DMN in CH_2Cl_2 rigid matrix at 77 K. The spectrum of **1**·$(H^+)_4$ is very similar to that of DMN.

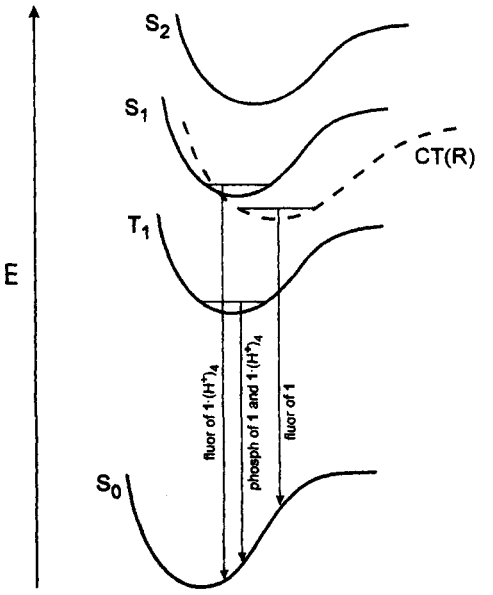

Figure 4. Schematic potential energy curves for the receptor **1** at room temperature. T_1, S_1, and S_2 are due to $\pi \rightarrow \pi^*$ transitions, whereas the charge-transfer (CT(R), where R stays for receptor) level is due to $n \rightarrow \pi^*$ transitions. In **1**·$(H^+)_4$, the CT(R) state is pushed to very high energy upon protonation of the amine groups. Therefore, the energy level diagram of **1**·$(H^+)_4$ is identical to that of 2,6-dimethylnaphthalene (DMN). Notice that the CT(R) level in rigid matrix at 77 K is not relaxed, and, as a consequence, the CT(R) curve should be raised in energy. For more details, see text.

phosphorescence band (Figure 3), which, as usual,[23] can only be seen in rigid matrix. In **1**, where the DMN units are covalently linked with the [18]-N_2O_4 crown ethers, a charge-transfer excited state originates because of the transition from the n orbitals of the amine moieties to the π^* orbitals of the aromatic rings. This state is distorted compared to the ground-state geometry, and its minimum is likely below the minimum of the S_1 level. The presence of this charge-transfer level in the receptor (hereafter indicated by CT(R))[24] accounts for the spectroscopic properties of **1**, i.e., (i) the presence of a broad absorption tail ($S_0 \rightarrow$ CT(R)), (ii) the lack of $S_1 \rightarrow S_0$ emission because of a fast $S_1 \rightarrow$ CT(R) deactivation, and (iii) the presence of a broad, low-energy emission (CT(R) $\rightarrow S_0$). Upon addition of acid, the n orbitals of the

(20) Ibemesi, J. A.; El-Bayoumi, M. A. *Photochem. Photobiol.* **1980**, *31*, 97.

(21) Beddard, G. S.; Davidson, R. S.; Whelan, T. D. *Chem. Phys. Lett.* **1977**, *56*, 54.

(22) (a) Oevering, H.; Paddon-Row, M. N.; Heppener, M.; Oliver, A. M.; Kotsaris, E.; Verhoeven, J. W.; Hush, N. S. *J. Am. Chem. Soc.* **1987**, *109*, 3258. (b) Schuddeboom, W.; Scherer, T.; Warman, J. M.; Verhoeven, J. W. *J. Phys. Chem.* **1993**, *97*, 13092.

(23) Gilbert, A.; Baggott, J. *Essentials of Molecular Photochemistry*; Blackwell: London, 1991.

(24) The charge-transfer level and the corresponding absorption and emission bands of the receptor **1** are indicated by the abbreviation CT(R) in order to distinguish them from the charge-transfer level and bands (CT(A)) that will be found later on in the adduct with $[Pt(NH_3)_2(bpy)]^{2+}$.

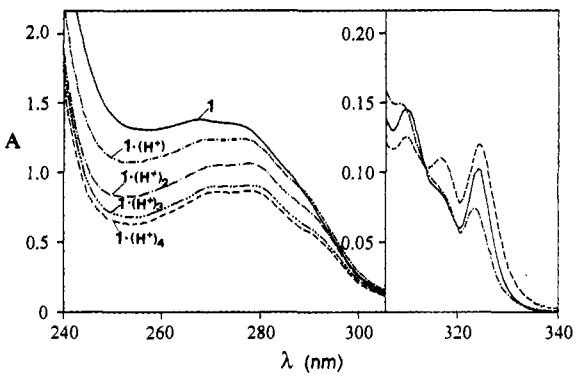

Figure 5. Changes in the absorption spectra observed upon addition of 1–4 equiv of CF_3COOH to a 1.2×10^{-4} M solution of **1** in CH_2Cl_2. On the right-hand side, the curves corresponding to $\mathbf{1}\cdot(H^+)_2$ and $\mathbf{1}\cdot(H^+)_3$ have been omitted for the sake of clarity.

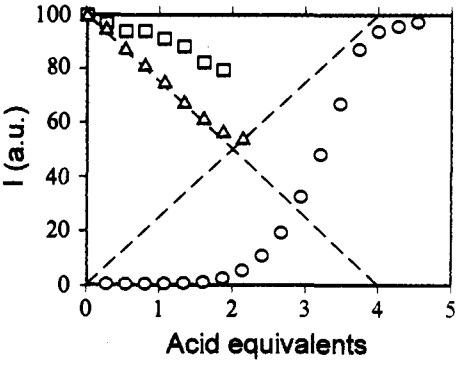

Figure 6. Changes in the intensities of the $\pi\pi^*$ fluorescence (342 nm, O) and of the CT(R) fluorescence (438 nm, Δ; 490 nm, □) upon addition of CF_3COOH to a 1.2×10^{-4} M CH_2Cl_2 solution of **1**. Excitation wavelength, 312 nm. The dashed lines indicate the changes that would be expected in the absence of interaction between the amine groups.

amine groups of **1** are engaged in proton coordination, and thus the CT level must move to much higher energy. In principle, a fluorescent excimer could be formed, but apparently the rigidity of the structure prevents the two rings from adopting a sandwich conformation. Therefore, at low energies, $\mathbf{1}\cdot(H^+)_4$ exhibits the same energy level pattern as DMN, and, as a consequence, its absorption and luminescence become practically identical to that of the reference chromophore.

In rigid matrix at 77 K, the CT(R) level of **1** is likely displaced to higher energy because of the lack of solvent repolarization. The CT(R) luminescence band, in fact, can be seen only as a tail covered by the S_1 luminescence, which, in its turn, has regained intensity because of the more difficult $S_1 \rightarrow$ CT(R) relaxation.

Spectroscopic Behavior of the Partially Protonated Forms of 1. The macrotricycle **1** exhibits a highly symmetric structure. Two DMN units are symmetrically linked to two identical macrocycles through two equivalent nitrogen atoms. The various subunits of **1** may interact with one another. For example, the four nitrogen atoms are structurally equivalent, but their protonation cannot occur independently because of through-space and through-bond interactions. When one of the four nitrogens is protonated, the second protonation will most likely involve the remote nitrogen of the other macrocycle rather than the second nitrogen of the same macrocycle or the second nitrogen of the same DMN unit. One can also expect that the spectroscopic properties of each subunit may be affected by the presence of a proton in a nearby unit. Therefore, upon progressive protonation of **1**, one cannot expect to observe smooth and monotonous changes from the spectra of **1** to those exhibited by the fully protonated $\mathbf{1}\cdot(H^+)_4$ form. This is clearly confirmed by the experimental results.

As shown in Figure 5, successive protonation of the four nitrogen atoms of **1** is in fact accompanied by complex changes in the absorption spectrum. The generalized decrease of intensity in the region of the CT(R) absorption tail (240–300 nm) is consistent with the disappearance of $n \rightarrow \pi^*$ transitions upon protonation of the nitrogen atoms. Such a decrease, however, is not linear and is more pronounced at shorter wavelengths (Figure 5). This shows that protonation of a nitrogen does not simply cancel the $n \rightarrow \pi^*$ transition in which that nitrogen is involved but also affects other $n \rightarrow \pi^*$ or $\pi \rightarrow \pi^*$ transitions. Protonation of one of the (donor) amine groups appended to a DMN chromophore is in fact expected to decrease slightly the energy of the $n \rightarrow \pi^*$ transition involving the nonprotonated nitrogen appended to the same chromophoric group because of the electron-withdrawing effect of the positive charge on the naphthalene ring. Therefore, upon addition of the first two protons, the CT(R) absorption tail is expected not only to decrease but also to move to the red, in agreement with the observed behavior. In the region of the ^1L_b $\pi \rightarrow \pi^*$ transition (Figure 5, λ = 320–340 nm), an initial decrease of the absorbance is followed by an increase at higher acid concentrations. This may reflect the decrease in the symmetry of the DMN chromophoric groups when only one of their appended amine units is protonated and the recovery of a higher symmetry upon complete protonation.

The interaction between the various subunits as protonation proceeds is extremely important for the luminescence properties. The presence of a quasiisosbestic absorption region around 312 nm (Figure 5) allowed us to choose an excitation wavelength capable of exciting the various species in proportion to their relative concentrations. In the absence of any interaction of the subunits, excitation at 312 nm would therefore cause a monotonous decrease of the intensity of the CT(R) luminescence band, with maximum at 438 nm accompanied by a corresponding increase in the intensity of the $\pi\pi^*$ fluorescence band with maximum at 344 nm (Figure 2), as indicated by the dashed lines in Figure 6. The experimental behavior, however, is quite different. The CT(R) band decreases from the beginning of protonation but with different gradients at different wavelengths. Such a decrease is not accompanied by the appearance of the $\pi\pi^*$ fluorescence. The latter band shows up only after the second protonation, displays a 50% intensity in correspondence of the $\mathbf{1}\cdot(H^+)_3$ form, and reaches a maximum after full protonation. The behavior of the CT(R) band can be followed only up to the second protonation, since at this point the appearance of the much more intense (Table 1) $\pi\pi^*$ fluorescence covers the residual CT(R) emission.

The observed behavior can be rationalized as follows. For each chromophoric moiety of **1**, the energy level diagram is that shown in Figure 4. Upon monoprotonation, nothing changes in one of the two chromophoric moieties. In the other chromophoric moiety, an amine group is protonated, but there is still a nonprotonated amine group, which assures the presence of a CT(R) level. Therefore, the $\pi\pi^*$ fluorescence cannot show up. Because of the protonation of one of the two amine groups, the CT(R) level of the monoprotonated chromophoric unit is expected to lie at lower energy than the original one, and it can also exhibit a different luminescence intensity. In fact, the CT(R) luminescence of the mono- and diprotonated forms becomes slightly red-shifted and less intense, which accounts for the different gradients of the intensity decrease on addition of acid (Figure 6). Upon addition of the third proton equivalent, one of the chromophoric units becomes fully protonated so that it does not contain any low-energy CT(R) level, and the $\pi\pi^*$ fluorescence can show up. At the third stage of protonation, only a red-shifted, weak CT luminescence is expected, but it cannot be seen because it is covered by the very strong $\pi\pi^*$ fluorescence.

Adducts with Cadaverine and Ammonium Ions. It is well known that **1** gives rise to a 1:2 adduct with NH_4^+ ions and to a 1:1 adduct with the cadaverine dication $NH_3^+(CH_2)_5NH_3^+$.[12a] The X-ray structure of the adduct of **1** with the cadaverine dication

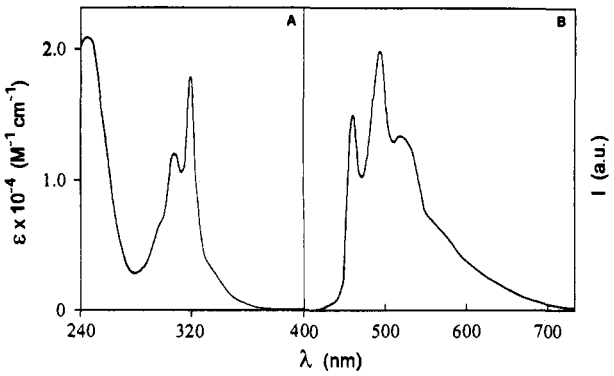

Figure 7. Absorption (A) and emission (B) spectra of $[Pt(NH_3)_2(bpy)]^{2+}$ (as [18]-O_6 adduct) in CH_2Cl_2 solution at room temperature.

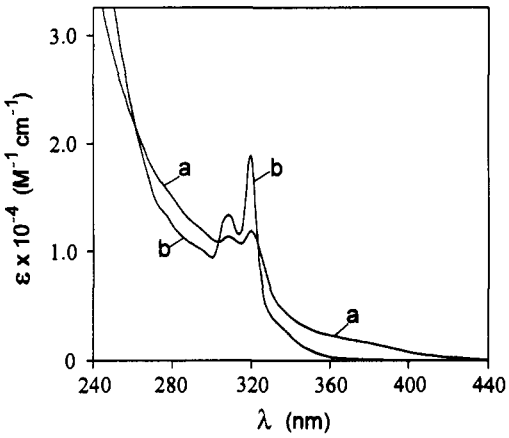

Figure 8. (a) Absorption spectrum of the 1:1 adduct of **1** and $[Pt(NH_3)_2(bpy)]^{2+}$ in CH_2Cl_2 solution at room temperature. (b) Summation of the spectra of the two components under the same experimental conditions.

reveals its cryptate-type nature, showing that the substrate is held inside the receptor molecule by simultaneous binding to the macrocyclic [18]-N_2O_4 subunits via hydrogen bonds.[12b]

Addition of solid NH_4PF_6 to a CH_2Cl_2 solution of **1** (1.0×10^{-4} M) or of solid $(NH_3^+(CH_2)_5NH_3^+)Cl_2$ to a CH_2Cl_2/MeOH (10:1, v/v) solution of **1** causes a decrease in the CT(R) absorption tail and a reduction of about 50% in the intensity of the CT(R) emission, with a very small increase of the $\pi\pi^*$ fluorescence intensity. These results are consistent with the formation of adducts of **1** with ammonium and cadaverine cations, where two NH_4^+ cations or one $NH_3^+(CH_2)_5NH_3^+$ dication are hosted in the macrotricycle cavity and are engaged in hydrogen bonds with macrocyclic nitrogens appended to different DMN units.[12]

Adduct with $[Pt(NH_3)_2(bpy)]^{2+}$. $[Pt(NH_3)_2(bpy)](PF_6)_2$ is not soluble in CH_2Cl_2, but it can be dissolved upon addition of [18]-crown-6 (hereafter called [18]-O_6) to give a 1:1 adduct.[16b] The absorption and emission spectra of this adduct in CH_2Cl_2 are practically identical to those of free $[Pt(NH_3)_2(bpy)]^{2+}$ in acetonitrile. This suggests that there is negligible electronic interaction between $[Pt(NH_3)_2(bpy)]^{2+}$ and [18]-O_6, which are associated through hydrogen bonds involving an amine ligand of the complex.[15] The absorption spectrum of $[Pt(NH_3)_2(bpy)]^{2+}$ (Figure 7) displays a quite intense absorption in the 290–340-nm region, with two peaks located at 308 and 319 nm, due to metal-perturbed transitions centered on the bpy ligand (hereafter indicated by LC(bpy)). At room temperature, the complex shows a structured emission (Figure 7) with a maximum at 488 nm and a lifetime of 100 ns (λ_{max} = 486 nm and τ = 25 μs at 77 K) that can be assigned to a formally spin-forbidden ^{3}LC(bpy) level.[16b]

When solid $[Pt(NH_3)_2(bpy)](PF_6)_2$ is added to a CH_2Cl_2 solution of **1**, an adduct is formed as shown by the absorption spectrum, which is noticeably different from the sum of the spectra

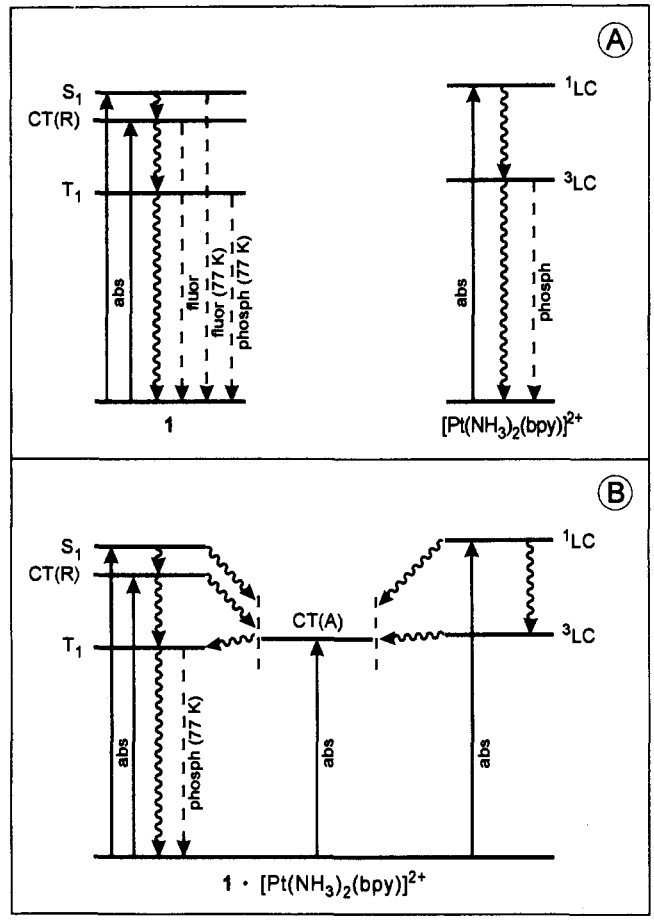

Figure 9. Schematic energy level diagrams for **1** and $[Pt(NH_3)_2(bpy)]^{2+}$ (A) and for their **1**·$[Pt(NH_3)_2(bpy)]^{2+}$ adduct (B).

of the two separated components (Figure 8). In particular, adduct formation causes a decrease in the intensity of the 319-nm band of the Pt complex and an increase in absorbance in the 320–420-nm region because of the presence of a shoulder at 375 nm (ϵ = 1800 M^{-1} cm^{-1}). By analogy with other similar adducts,[16b] this shoulder can be assigned to a charge-transfer transition in the adduct (CT(A)) involving the electron-rich DMN units and the electron-deficient bpy ligand of the $Pt(bpy)^{2+}$ moiety. Upon adduct formation, profound changes are also observed in the luminescence spectra. At room temperature, both the CT(R) band of **1** (λ_{max} = 438 nm, Figure 2) and the ^{3}LC(bpy) band of the Pt complex (λ_{max} = 488 nm, Figure 7) disappear, and no other luminescence band is present. At 77 K, the ^{3}LC(bpy) band of the Pt complex and the fluorescence band of **1** disappear again, but the phosphorescence band of **1** (Figure 3) is present and can be observed even upon excitation in the absorption bands centered on $[Pt(NH_3)_2(bpy)]^{2+}$. It is also noteworthy that, in the adduct, the lifetime of the phosphorescence emission of **1** is much shorter than that in free **1** (Table 1). As suggested by observation of CPK models, the above results indicate that the $[Pt(NH_3)_2(bpy)]^{2+}$ complex is hosted in the cylindrical cavity of **1**, with an amine ligand involved in hydrogen bonds with a crown and the flat $Pt(bpy)^{2+}$ moiety sandwiched between the two DMN chromophoric groups. The adduct charge-transfer excited state, CT(A), lies certainly below the S_2, S_1, and CT(R) levels of **1**, as well as below ^{1}LC(bpy) level of the Pt complex. Although the exact position of the zero–zero level of the CT(A) excited state is not known, from the extension of the corresponding absorption tail to low energy (perhaps 440–450 nm, Figure 8), such a level appears to be very close (perhaps below) to the zero–zero level of the ^{3}LC(bpy) excited state of the Pt complex, which, in its turn, is just above the phosphorescent T_1 state of **1** (Figures 3 and 7). The overall energy level situation for the **1**·$[Pt(NH_3)_2(bpy)]^{2+}$

adduct can therefore be summarized as in Figure 9. One can then understand that, in the adduct, the fluorescence of the free receptor is quenched because the receptor-localized S_1 and CT(R) levels undergo fast radiationless decay to the adduct charge-transfer level, CT(A). On the other side, the substrate-localized ^{3}LC(bpy) level is quenched by the T_1 or even by the CT(A) level. In its turn, the CT(A) level may be quenched by T_1, which, at least at 77 K, is the lowest excited state of the adduct, since its emission can be observed in rigid matrix. The strong decrease in the excited-state lifetime of the T_1 emission in passing from free **1** (2.6 s) to its adduct with the Pt complex (8×10^{-4} s) can be accounted for by the perturbation induced on the formally spin-forbidden $T_1 \rightarrow S_0$ transition by mixing of the T_1 level with the nearby CT(A) level which involves the heavy Pt atom.

Acknowledgment. We would like to thank Prof. J. W. Verhoeven for stimulating discussion, Miss C. Francioni for some preliminary experiments, and Mr. L. Minghetti and Mr. G. Gubellini for technical assistance. This work was supported by the Ministero dell'Università e della Ricerca Scientifica e Tecnologica (MURST), Consiglio Nazionale delle Ricerche (CNR), and the Centre National de la Recherche Scientifique (CNRS).